

Evaluation of Hydrogen-Induced Blistering of Mo/Si Multilayers with a Capping Layer

Hiroaki TOMURO^{1,2)}, Mengran JI¹⁾, Ryo NAGATA¹⁾, Koichiro KOUGE^{1,2)}, Tatsuya YANAGIDA²⁾, Masayuki MORITA²⁾, Masahiko ANDOU²⁾, Yoshiyuki HONDA²⁾, Kiichiro UCHINO¹⁾ and Tsuyoshi YOSHITAKE¹⁾

¹⁾*Interdisciplinary Graduate School of Engineering Sciences, Kyushu University, Kasugakoen, Kasuga, Fukuoka 816-8580, Japan*

²⁾*Gigaphoton Inc. Hiratsuka facility, Shinomiya, Hiratsuka, Kanagawa 254-8567, Japan*

(Received 30 September 2021 / Accepted 20 January 2022)

Mo/Si multilayer mirrors are used for extreme ultraviolet (EUV) lithography. The formation of hydrogen-induced blisters in the Mo/Si multilayer is a problem that reduces the reflectance of the mirror. To evaluate the blister-resistance of EUV mirrors, the blister formation processes of Mo/Si multilayers with a capping layer were investigated using a high-frequency hydrogen plasma system as a hydrogen ion source under varying hydrogen ion exposure conditions. As a result, it was observed that blister formation by low-energy hydrogen ion irradiation of about 10 eV increases the blister-occupied area, depending on the amount of the ion dose. Furthermore, the sample was heated to promote the diffusion of hydrogen atoms, and the activation energy of blister formation was examined using the Arrhenius plot of the ion dose required for blister formation with respect to the heating temperature. The analysis showed that when the ion flux is known, the blister formation time can be predicted.

© 2022 The Japan Society of Plasma Science and Nuclear Fusion Research

Keywords: EUV lithography, Mo/Si multilayer, capping layer, CCP plasma, blister

DOI: 10.1585/pfr.17.1406005

1. Introduction

It is well known that exposure to hydrogen and helium ions forms blisters on fusion reactor walls, causing metal impurity contamination of the fusion plasma [1–4]. Similar problems occur with collector mirrors in extreme ultraviolet (EUV) lithography systems [5–9]. The collector mirror has a Mo/Si multilayer on the surface to reflect and condense EUV radiation at a wavelength of 13.5 nm, and its reflectivity is approximately 70% [7, 10]. This reflectivity must be maintained during the operation of EUV systems with hundreds of billions of shots or more. Hydrogen gas flows into the vessel of the EUV lithography system at a pressure in the order of 10 Pa to maintain the cleanliness of the inner wall of the vessel and the surface of the collector mirror. Hydrogen gas is activated by EUV radiation to generate hydrogen ions and radicals. The hydrogen ions and radicals react with contaminants in the vessel, and the formed hydrogenated gas is exhausted to the outside of the vessel. However, the hydrogen induces blistering in the Mo/Si multilayer mirrors [11–17]. The mechanism of blister formation is as follows [14, 18, 19]. Hydrogen atoms permeated into the multilayer are trapped in the defects at the layer boundary, where they recombine into hydrogen molecules. When the amount of hydrogen atoms is sufficiently permeated, hydrogen molecules accumulate causing high pressure to form blister. Hydrogen-induced blister

formation shortens the lifetime of Mo/Si multilayer mirrors and causes a decrease in availability of EUV lithography. Therefore, elucidation of the relationship between blister formation periods and hydrogen exposure conditions is important for EUV lithography development. Most previous research on blistering focused on Mo/Si multilayer mirrors without a capping layer [11–17]. However, the Mo/Si multilayer on EUV mirrors must include a capping layer on top of the multilayer to prevent oxidation and damage from tin debris [20–24]. Blistering formation on the Mo/Si multilayer with a capping layer was reported in [20], though the dependence on exposure conditions was not clear.

In this study, we investigated the blister resistance of Mo/Si multilayers with a capping layer. In the actual EUV light source vessel, as described above, the hydrogen gas in the vessel is ionized by EUV light, and plasma with an electron density of $\sim 10^{16} \text{ m}^{-3}$ and a lifetime of several μs is generated with high repetition (10 - 100 kHz) near the surface of the EUV mirror [6]. The high photon energy (93 eV) of EUV light may form relatively high-energy electrons and ions, but these high-energy ions and electrons are thermally relaxed in about 10 ns. Finally, the ion temperature approaches the gas temperature and the electron temperature becomes 1 - 2 eV. A hydrogen ion sheath is formed on the mirror surface. As described in Sec. 3, the voltage applied to the sheath is about three times the electron temperature. Therefore, hydrogen ion irradiation

author's e-mail: hiroaki_tomuro@global.komatsu

on the mirror surface from plasma is dominated by low-energy ions of 10 eV or less.

It is difficult to evaluate the blister formation process directly using an EUV lithography system because the multilayer is affected by the oxidation and damaged by the tin debris. For this reason, we attempted to investigate the blister formation process using systems of capacitively coupled plasmas (CCP) of radio frequency (RF, 13.56 MHz) and very high frequency (VHF, 30 MHz). The blister formation depends on exposed hydrogen ion energy, sample temperature, and ion dose. The self-bias voltage that appears in the powered electrode of the CCP plasma was used to generate high-energy hydrogen ions. Multilayer samples with and without a capping layer were placed on the powered electrode and irradiated with high-energy hydrogen ions, and the difference in the blister formation process between the two cases was investigated. For low-energy hydrogen ion exposure, the blister formation process was investigated with samples fixed on a ground electrode. In this case, the diffusion process of hydrogen atoms in the sample is important for blister formation, hence this ground electrode was provided with a mechanism that enables heating up to 180°C. The results showed that the blister formation time can be estimated based on the temperature of the Mo/Si multilayer mirror sample with a capping layer, which leads to the prediction of the lifetime of the mirror.

2. Experimental Setup and Methods

Samples used in this experiment had multilayer stacks consisting of 60 Mo/Si bilayers deposited on a polished Si (100) substrate (surface roughness was ~ 0.2 nm). The samples were $7 \times 7 \times 0.6$ mm³ and a pair of Mo/Si layers was about 7 nm thick. For the investigation, two types of multilayer samples were prepared: one was capped with a metal oxide layer and the other was uncapped.

The multilayer samples were exposed to hydrogen ions by the CCP. A schematic of the hydrogen CCP system is shown in Fig. 1. The vacuum exhaust port was located at 90° in the same plane as the gas filling port of the vacuum vessel. The ultimate pressure in the vacuum vessel was $\sim 2 \times 10^{-2}$ mTorr. The hydrogen plasma generation conditions were an RF discharge (13.56 MHz) with a hydrogen pressure of 100 mTorr and a VHF discharge (30 MHz) with a hydrogen pressure of 500 mTorr. The hydrogen gas flow rate and supply power were 60 sccm and 20 W. The electron density (n_e) and electron temperature (T_e) were measured using a Langmuir probe to evaluate the ion flux on the sample surface [25]. The measuring part of the probe tip was columnar tungsten with a length of 10 mm and a diameter of 0.5 mm. For the high energy hydrogen ion exposure, multilayer samples were exposed to hydrogen ions by placing them on top of the powered electrode (diameter = 80 mm) of the RF discharge. The samples were exposed to hydrogen ions accelerated by a negatively self-

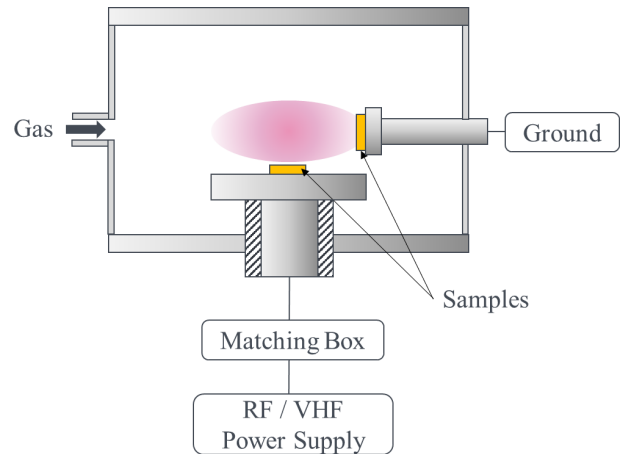


Fig. 1 Schematic of the capacitively coupled plasma (CCP) device for hydrogen exposure.

biased voltage. The self-bias voltage and voltage waveform were measured with a high voltage probe. The energy distribution of hydrogen ions was calculated using a simple mechanical model of acceleration by an electric field and collisions between particles. The temperature of the powered electrode was measured by a thermocouple attached from the atmosphere side. The temperature of the sample fixed to the powered electrode was assumed to be equal to the electrode temperature. For investigating the process of blister formation by the low-energy ion exposure, the sample was placed on the ground electrode (diameter = 24 mm) inserted from the side of the vacuum vessel toward the plasma on the powered electrode, as shown in Fig. 1. In this case, the sample is exposed to voltage-accelerated ions generated in the ion sheath formed on the ground electrode. A heating option was provided on this ground electrode. The electrode was heated by a heater, the temperature was measured by a thermocouple, and the on/off switch of the heater was controlled to maintain a constant heating temperature. The sample temperature during hydrogen ion exposure was varied in the range of 50 - 180°C. The maximum temperature control error was $\pm 5^\circ\text{C}$. Blisters in the samples were characterized by a high-resolution scanning electron microscope (SEM, JEOL, JSM-6510LA) and a transmission electron microscope (TEM, JEOL, JEM-ARM200F). Hydrogen depth profiles were measured by secondary ion mass spectrometry (SIMS, PHI, ADEPT-1010) to verify hydrogen implantation.

3. Results and Discussion

3.1 Exposure of samples to RF discharge

The plasma parameters of the RF discharge were measured from the probe currents in the same phase of the RF period for each probe voltage. The evaluated values of n_e and T_e were $1 \times 10^{15} \text{ m}^{-3}$ and 2.1 eV. Figure 2 shows typical SEM images of the surface of the multilayer sam-

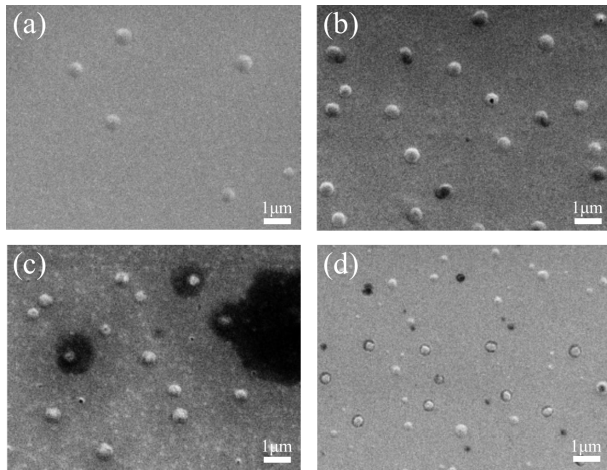


Fig. 2 Typical SEM images of blisters in Mo/Si multilayers with a capping layer. Exposure times were (a) 10 min, (b) 20 min, (c) 40 min, and (d) 80 min. The hydrogen plasma was produced by RF discharge at a frequency of 13.5 MHz.

Table 1 Hydrogen exposure conditions for RF discharge and blister coverages by SEM measurements.

Sample capping layer	Exposure time [min]	Sample temperature [°C]	Ion dose [m ⁻²]	Blister area ratio [%]
Yes	10	35	3.1×10^{21}	1.4
Yes	20	42	6.2×10^{21}	5.0
Yes	40	49	1.3×10^{22}	3.5
Yes	80	49	2.5×10^{22}	5.6

ples with a capping layer after hydrogen exposure with the RF discharge, with exposure times of (a) 10 min, (b) 20 min, (c) 40 min, and (d) 80 min. Table 1 shows the exposure conditions and blister area ratio obtained from the SEM images. The ion dose in Table 1 is evaluated by the exposure time n_e and the Bohm velocity of ions at the sheath end formed on the surface of the powered electrode; the Bohm velocity is given by $(\kappa T_e / M_i)^{0.5}$, where κ is the Boltzmann constant, T_e is the electron temperature in K, and M_i is the mass of the ion. According to Ref. [26], under the experimental conditions in this study, most of the hydrogen ions are H_3^+ . As shown in Table 1, the 20-min exposure of Fig. 2 (b) increased the blister area ratio compared to the 10-min exposure of Fig. 2 (a). However, in the 40-min exposure of Fig. 2 (c), the blister area ratio decreased and a black area showing non-uniformity of the surface layer appeared. In Fig. 2 (d), the blister area ratio increased again. Regarding this series of changes, it can be understood that the capping layer disappeared completely by ion sputtering between 20 and 80 min, and blisters observed at 80 min were newly formed in the Mo/Si multilayer after the disappearance of the capping layer. Additionally, the sample temperature changed to 35°C at 10 min

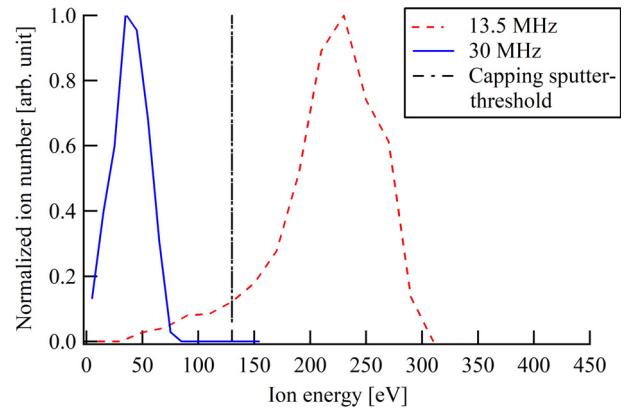


Fig. 3 Calculated ion energy distribution for RF discharge at 13.5 MHz (gas pressure 100 mTorr) and VHF discharge at 30 MHz (500 mTorr).

and 49°C at 40 min and above. The cause seems to be heating caused by the impact of the hydrogen ion beam. It has been reported in Ref. [14] that the blister area increases as the sample temperature rises, and the correlation between hydrogen ion dose and hydrogen blister formation becomes unclear. Therefore, it can be concluded that RF discharge is not suitable for the investigation of the blister resistance of the capping layer because the capping layer disappears owing to ion impact sputtering at the same time that the sample is heated.

To investigate whether the ion energy distribution of the RF discharge causes sputtering of the capping layer, the kinetic energy distribution of the ions on the electrode surface was calculated. For comparison, the same calculation was performed for the VHF discharge with a frequency of 30 MHz. The model was calculated using the Monte Carlo method until the ions starting from the sheath end reached the electrode surface while repeating elastic collisions with hydrogen molecules in an oscillating electric field that had a negative self-bias voltage. From the measurement of each discharge using the high voltage probe, the self-bias voltage of the RF discharge was -250 V and the self-bias voltage of the VHF discharge was -55 V. The amplitude of the discharge voltage waveform is only a few volts higher than these bias voltages. Here, the incident ion was calculated as H_3^+ , as described above. Figure 3 shows the calculation results, from which it can be seen that most ions have an energy of 200 - 300 eV in the case of the RF discharge. The sputtering of the capping layer at this energy was investigated with the TRIM code [27]. H_3^+ ions exist only in the gas phase and contribute as a neutral H_2 or H atom in collision cascade formation in solids. As a result, in the case of RF discharge, the capping layer may disappear by sputtering in several tens of minutes. In contrast, in the case of VHF discharge, most of the ion energy was 70 eV or less, and the sputtering yield calculated by the TRIM code was less than a few hundredths of

that in the case of RF discharge. Consequently, the blister resistance can be evaluated correctly by using the VHF discharge plasma, as sputtering of the capping layer is not a problem.

3.2 Exposure of samples on the powered electrode to VHF discharge

The Langmuir probe measurement of VHF discharge plasma used the method described in Ref. [25]. As a result, n_e was evaluated as $3.7 \times 10^{15} \text{ m}^{-3}$ and T_e was evaluated as 2.9 eV. Figure 4 shows typical SEM images of the multilayer sample surfaces after the VHF hydrogen plasma exposure on the powered electrode. Figures 4 (a) and (b) depict the samples with and without a capping layer, respectively, after a 4-h exposure. The formation of a blister with a maximum diameter of 15 μm or more was observed in Fig. 4 (a). This blister was formed at the boundary between the capping layer and the Mo/Si multilayer (See Fig. 7 (a) in the next section). Contrarily, no blister formation was observed in the sample without a capping layer. Table 2 shows the plasma exposure conditions and blister area ratios obtained from the SEM images. In addition, the sample temperature did not rise, remaining at 25°C, which matched the room temperature. The blisters in the capped sample took 1 h to form; however, the blister area ratio did not increase over 1 h, as shown in Table 2. From this result, the effect of these blisters on the reflectance of the mirror is limited. Although the blister area ratio is largest when the exposure time is 1 h in Table 2, this is caused by the variation and does not imply that the blister area ra-

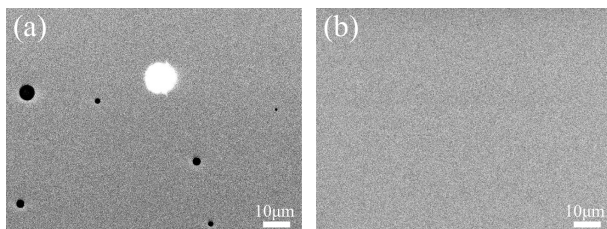


Fig. 4 Typical SEM images of blisters in Mo/Si multilayers, (a) with capping layer and (b) without capping layer. The hydrogen plasma was produced by RF discharge at a frequency of 30 MHz.

Table 2 Hydrogen exposure conditions for the VHF discharge and blister coverages by SEM measurements.

Sample capping layer	Exposure time [h]	Sample temperature [°C]	Ion dose [m^{-2}]	Blister area ratio [%]
Yes	1	25	1.4×10^{23}	3.5
Yes	2	25	2.7×10^{23}	2.0
Yes	4	25	5.4×10^{23}	1.3
No	4	25	5.4×10^{23}	0

tio decreases after 1 h. We consider that the reason why the blister area ratio does not increase with time is that a channel for passing hydrogen, such as a microcrack, is formed on the blister, causing hydrogen gas to be released from the channel. The blister in this case occurs in a defect between the capping layer and Mo/Si multilayer, and it is considered that the defect is formed by high-energy ions. The multilayer without the capping layer had no blister formation and showed high blister resistance, although it was exposed to a higher hydrogen-ion dose than the experiment in Ref. [17]. Even if the Mo/Si multilayers have the same structure, the blister resistance differs depending on the layer formation conditions of the multilayer. We considered that the multilayer in this study had fewer defects than that in Ref. [17] because of the progress of layer formation technology.

3.3 Exposure of samples on the ground electrode to VHF discharge

In this section, we discuss the results of exposure to hydrogen plasma by arranging the multilayer sample on the ground electrode inserted from the side of the vessel toward the plasma, as shown in Fig. 1. As the plasma is the same as that in Sec. 3.2, its parameters are $n_e = 3.7 \times 10^{15} \text{ m}^{-3}$ and $T_e = 2.9 \text{ eV}$. The surface of the multilayer sample, with or without capping, is an insulating wall. A sheath is formed between the surface of the insulating sample and the plasma. The voltage applied to this sheath is determined by the mass ratio of ions (H_3^+) and electrons and the electron temperature [28]. In this case, the sheath voltage is 10 V, which is obtained by multiplying the electron temperature in eV units by 3.4. Accordingly, the energy of hydrogen ions (H_3^+) that pass through the sheath from the hydrogen plasma and enter the surface of the multilayer sample is 10 eV.

Typical SEM images of multilayer samples exposed to plasma on the ground electrode are shown in Fig. 5 (a) for the case with the capping layer, and Fig. 5 (b) for the case without the capping layer. The conditions for both are a heating temperature of 150°C and an exposure time of 4 h. In the sample with the capping layer, blisters with a size of approximately 1 μm are clearly formed. Even when the

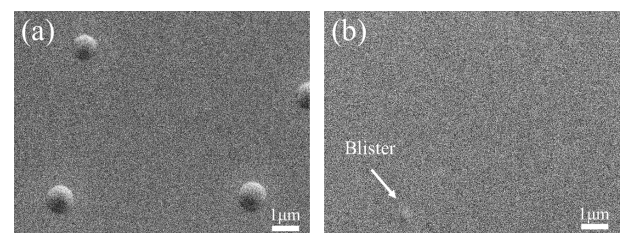


Fig. 5 Typical SEM images of blisters in Mo/Si multilayers on ground electrode with 4-h exposure and 150°C heating (a) with capping layer, (b) without capping layer.

Table 3 Hydrogen exposure on the ground electrode with the heating system and blister coverages by SEM measurements.

Sample capping layer	Exposure time [h]	Sample temperature [°C]	Ion dose [m ⁻²]	Blister area ratio [%]
Yes	4	50	5.4×10^{23}	0
Yes	4	100	5.4×10^{23}	0.9
Yes	4	150	5.4×10^{23}	2.0
Yes	4	180	5.4×10^{23}	3.5

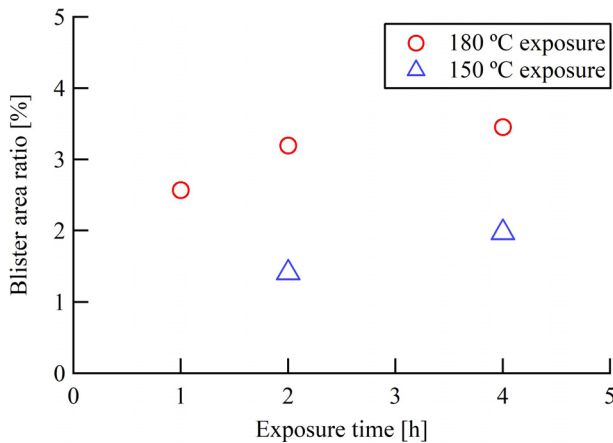


Fig. 6 Plots of blister area ratio versus exposure time on ground electrode with 150°C and 180°C heating.

sample was exposed to plasma on the ground electrode, blisters were more likely to form in the multilayer with the capping layer than in that without the capping layer, as was the case on the powered electrode. In the image without the capping layer, one small blister was exceptionally observed.

Table 3 shows the exposure conditions of the experiments on the ground electrode and the blister area ratios measured from the SEM images. For hydrogen exposure on the ground electrode, it is unlikely that ions with a low energy of 10 eV formed defects. Therefore, it is presumed that the cause is the damage generated during the sputter film formation of the capping layer. From Table 3, it can be seen that the blister area ratio increases as the heating temperature increases, even with the same exposure time. From this fact, it can be seen that hydrogen permeation is promoted by heating.

Figure 6 is a graph showing the relationship between the exposure time and blister area ratio when heated at 150°C and 180°C. The blister area increases as the exposure time increases, as opposed to the case on the powered electrode. To compare the details of the blister formation position and size when exposed on the ground and powered electrodes, the cross section of the sample surface after exposure was examined by TEM analysis. Fig-

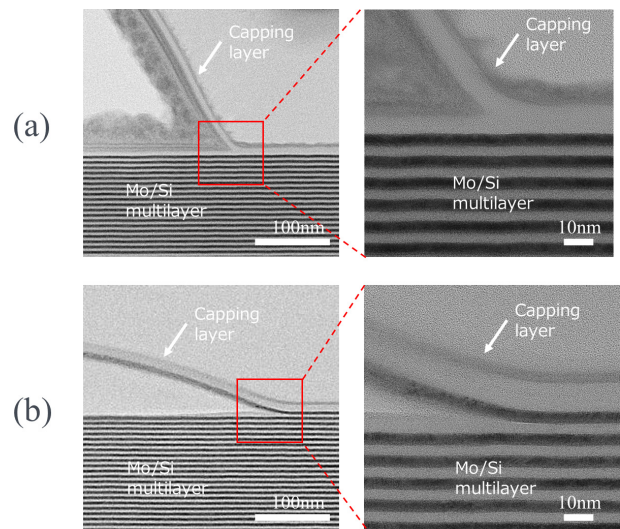


Fig. 7 Cross-sectional TEM images of blisters in Mo/Si multilayers with capping layer: (a) 4-h exposure on the powered electrode, (b) 4-h exposure with 150°C heating on the ground electrode.

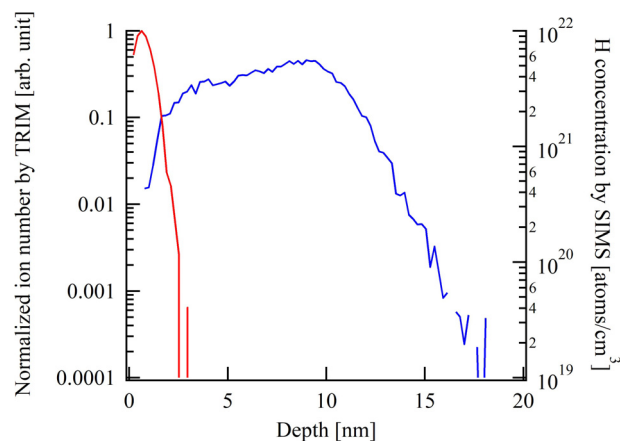


Fig. 8 Hydrogen concentration by SIMS measurement (blue line) and calculations by the TRIM code (red line).

ure 7 (a) shows a TEM image of the sample with the capping layer exposed to plasma for 4 h on a powered electrode (the same sample as Fig. 4 (a)), and Fig. 7 (b) shows a TEM image of the sample with the capping layer exposed to plasma for 4 h with heating at 150°C on the ground electrode (the same sample as in Fig. 5 (a)). In Fig. 7 (a), the blister was formed under the capping layer, whereas in Fig. 7 (b), it was formed under the first Mo layer in the Mo/Si multilayer. In Ref. [17], it was shown that a blister formed under the Mo layer in which hydrogen does not easily pass through in the Mo/Si multilayer. Similarly, in this study, we confirmed that the blister in the multilayer sample placed on the ground electrode was formed under the Mo layer, as shown in Fig. 7 (b), not under the capping layer where hydrogen easily passed through.

Figure 8 shows the hydrogen depth profile measured by SIMS when the sample with the capping layer was heated to 50°C and exposed to 10-eV ions (blue line), and the depth profile calculated 10-eV ion penetration by the TRIM code (red line). Through SIMS, a high hydrogen concentration was measured up to a depth of 18 nm, although TRIM calculations show that hydrogen ions only reach a depth of 2 - 3 nm. These suggest that blisters are formed by accelerating hydrogen penetration by heating.

Thermal diffusion of hydrogen atoms is considered to be the main mechanism of blister formation in thin films, and in Ref. [29], the activation energy for blister formation was obtained by using the Arrhenius plot. Similarly, as shown in Fig. 9, the hydrogen ion dose required to form blisters in the capped sample was Arrhenius plotted against the heating time. The hydrogen ion dose was calculated by multiplying the hydrogen ion flux ($3.8 \times 10^{19} \text{ m}^{-2} \text{ s}^{-1}$) by the time until a blister was formed. From the figure, the activation energy is about 0.3 eV (3550 K in the figure). When the sample temperature is 50°C ($1000/T = 3.1 \text{ K}^{-1}$), the hydrogen ion dose that forms the blister is read as $2 \times 10^{24} \text{ m}^{-2}$ on the extension of the broken line in the figure. According to Ref. [6], the hydrogen ion flux generated by EUV light is about $4 \times 10^{18} \text{ m}^{-2} \text{ s}^{-1}$. Assuming that this hydrogen ion flux is incident on a collector mirror made of a multilayer with the same properties as that used in this study under a surface temperature condition of 50°C, the blister formation time is estimated to be 137 h.

As aforementioned, the blister formation time was determined by the dose amount of hydrogen ions. Here, we describe the contribution of hydrogen atoms to the formation of blister. First, we estimate the hydrogen atom flux incident on the surface of the ground electrode inserted into the VHF plasma. A bright disk-shaped plasma region with a thickness of about 10 mm is formed on the electrode with a cathode sheath (thickness: 10 mm) in between. Because of the occurrence of the electron im-

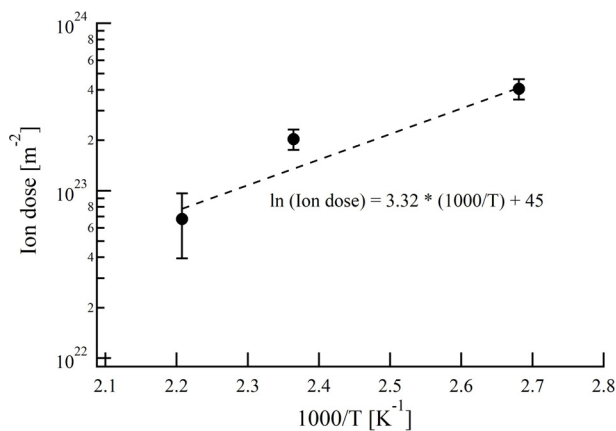


Fig. 9 Arrhenius plot of blister formation ion dose as a function of reciprocal temperature of multilayer samples with capping layer.

pact dissociation of hydrogen molecules, the generation rate of hydrogen atoms is calculated. The value is determined by the product of hydrogen molecular density at 500 mTorr (the gas temperature is assumed at 400 K), electron density ($3.5 \times 10^{15} \text{ m}^{-3}$), rate coefficient of dissociation ($2 \times 10^{15} \text{ m}^3 \text{ s}^{-1}$ at $T_e = 2.9 \text{ eV}$ [30]), and volume of this region. The loss rate of hydrogen atoms is determined by the diffusion of hydrogen atoms to the surface of the electrode 10 mm away, where they are adsorbed or recombined. The hydrogen atom density, which is determined by the balance between the generation and loss of hydrogen atoms, is about $1 \times 10^{19} \text{ m}^{-3}$. When a thermal velocity of 400 K is applied, the flux of hydrogen atoms incident on the multilayer sample on the ground electrode becomes $3 \times 10^{22} \text{ m}^{-2} \text{ s}^{-1}$. Hydrogen atoms are chemically adsorbed on the solid surface. The adsorbed hydrogen atoms must exceed a potential barrier on the order of 1 eV to penetrate into the solid [31]. Kuznetsov et al. conducted comparative experiments on the formation of blister on Mo/Si multilayers for a mixed flux of hydrogen atoms and hydrogen ions and a flux of only atoms [14]. According to the results, the penetration rate of hydrogen atoms was about 10^{-5} of hydrogen ions at the multilayer temperature of 200°C. Considering the results, the flux of hydrogen atoms that actually permeated into the Mo/Si multilayer in this study was $3 \times 10^{17} \text{ m}^{-2} \text{ s}^{-1}$. Compared to the aforementioned hydrogen ion flux, the hydrogen atom flux was on the order of 1% and was negligible.

4. Conclusion

This study demonstrated that VHF plasma can be used to evaluate the blister resistance of multilayer samples with a capping layer for EUV mirrors. In particular, by using the powered electrode and the ground electrode, it was suggested that the blister formation process differs depending on the ion energy incident on the sample. Furthermore, in the formation of blisters by hydrogen ion exposure with low ion energy, the Arrhenius plot of the ion doses with respect to the heating temperature suggested that the blister formation time can be predicted.

In the current EUV lithography system, debris deposition and oxidation of the mirror surface determine the decrease in reflectance of the mirror. The capping layer is formed on the mirror surface as a countermeasure for the decrease; however, it was found in this study that the capping layer reduces the blister resistance of the Mo/Si multilayer. It is expected that the method used in this study will be used to evaluate blister resistance for various types of capping layers and film formation methods, and that an optimal capping layer will be developed.

- [1] A.F. Bardamid *et al.*, Plasma Devices Oper. **14**, 159 (2006).
- [2] V.K. Alimov *et al.*, J. Nucl. Mater. **381**, 267 (2008).
- [3] H.Y. Xu *et al.*, Nucl. Mater. **443**, 452 (2013).
- [4] Y. Uchida *et al.*, Plasma Fusion Res. **13**, 1205084 (2018).

- [5] T. Yamazaki *et al.*, H. Proc. SPIE **9422**, 94222 (2015).
- [6] M. van de Kerkhof *et al.*, Proc. SPIE **11323**, 113230 (2020).
- [7] A. Endo, J. Mod. Phys. **5**, 285 (2014).
- [8] A. Dolgov *et al.*, J. Phys. D, Appl. Phys. **47**, 065205 (2014).
- [9] D.T. Elg *et al.*, Plasma Chem. Plasma Process. **38**, 223 (2018).
- [10] S. Braun *et al.*, Jpn. J. Appl. Phys. **41**, 4082 (2002).
- [11] A.S. Kuznetsov *et al.*, Proc. SPIE **8077**, (2011).
- [12] A.S. Kuznetsov *et al.*, J. Phys. Condens. Matter. **24**, 052203 (2012).
- [13] A.S. Kuznetsov *et al.*, J. Appl. Phys. **114**, 113507 (2013).
- [14] A.S. Kuznetsov *et al.*, J. Appl. Phys. **115**, 173510 (2014).
- [15] R.A.J.M. van den Bos *et al.*, J. Appl. Phys. **120**, 235304 (2016).
- [16] R.A.J.M. van den Bos *et al.*, J. Phys. D: Appl. Phys. **50**, 265302 (2017).
- [17] R.A.J.M. van den Bos *et al.*, J. Phys. D: Appl. Phys. **51**, 115302 (2018).
- [18] F. Okba *et al.*, Appl. Phys. Lett. **97**, 031917 (2010).
- [19] L. Shao *et al.*, Appl. Phys. Lett. **87**, 091902 (2005).
- [20] D.T. Elg *et al.*, J. Vac. Sci. Technol. A **34**, 021305 (2016).
- [21] S. Bajt *et al.*, Proc. SPIE **5037**, Emerging Lithographic Technologies VII (2003).
- [22] N. Benoit *et al.*, Appl. Opt. **47**, 3455 (2008).
- [23] T. Feigl *et al.*, Proc. SPIE **8679**, 86790 (2013).
- [24] R.C. Ribera *et al.*, Appl. Phys. **188**, 055303 (2015).
- [25] K. Kato *et al.*, J. Math. Phys. **4**, 1811 (2016).
- [26] L. St-Onge *et al.*, Plasma Chem. Plasma Process. **14**, 87 (1994).
- [27] W. Takeuchi *et al.*, Radiat. Eff. **71**, 53 (1983).
- [28] M.A. Lieberman and A.J. Lichtenberg, *Principles of Plasma Discharges and Materials Processing, 2nd ed.* (Wiley, Hoboken, NJ, 2005).
- [29] R. Singh *et al.*, J. Electron. Mater. **39**, 2177 (2010).
- [30] K. Sawada, J. Appl. Phys. **78**, 2913 (1995).
- [31] A. Züttel, Mater. Today Commun. **6**, 24 (2003).